Kinetic Model of the Partial Oxidation of Methane to Synthesis Gas Over Ru/TiO_2 Catalyst

Costas Elmasides, Theophilos Ioannides, and Xenophon E. Verykios
Dept. of Chemical Engineering, University of Patras, GR-265 00 Patras, Greece

The kinetic behavior of the Ru/TiO_2 catalyst in the partial oxidation of methane to synthesis gas was investigated as a function of temperature and partial pressures of CH_4 and O_2. It was found that the catalyst promotes, to a large extent the direct formation of CO and H_2 from the reaction of methane and oxygen, while the reforming and water − gas shift reactions are negligible under these conditions. A kinetic model, based on formation of CO and H_2 as primary products and of CO_2 and H_2O as secondary oxidation products, describes satisfactorily the observed kinetic behavior. Values of model parameters satisfy thermodynamic constraints and agree well with data derived from surface science techniques and kinetic studies of elementary surface processes that are in the literature.

Introduction

Formation of synthesis gas via catalytic partial oxidation of methane has received significant attention during the past several years. A review of the process and its comparison with existing technologies for syngas production has been published (Pena et al., 1996).

Concerning the reaction pathway of the partial oxidation of methane to synthesis gas, two main reaction schemes have been proposed: one is the sequence of total oxidation followed by reforming reactions (indirect scheme, Eqs. 2–4), and the other is the direct conversion of methane to synthesis gas without the formation of CO_2 and H_2O as reaction intermediates (direct scheme, Eq. 1).

$$CH_4 + \frac{1}{2}O_2 \rightarrow 2H_2 + CO \qquad \Delta H_{298}^{o} = -35 \text{ kJ/mol} \qquad (1)$$

$$CH_4 + 2O_2 \rightarrow CO_2 + 2H_2O \qquad \Delta H_{298}^{o} = -801 \text{ kJ/mol} \qquad (2)$$

$$CH_4 + CO_2 \rightarrow 2CO + 2H_2 \qquad \Delta H_{298}^{o} = +247 \text{ kJ/mol} \qquad (3)$$

$$CH_4 + H_2O \rightarrow CO + 3H_2 \qquad \Delta H_{298}^{o} = +206 \text{ kJ/mol} \qquad (4)$$

Correspondence concerning this article should be addressed to X. E. Verykios.
Present address of T. Ioannides: Foundation for Research and Technology—Hellas (FORTH), Institute of Chemical Engineering and High Temperature Chemical Processes (ICE/HT), P.O. Box 1414, GR-265 00 Patras, Greece.

The indirect scheme is supported by experimental findings of several investigators, who have shown that a considerable hot spot develops at the entrance of the catalytic bed. This is indicative of the occurrence of the exothermic methane combustion. In this case, CO and H_2 selectivity are practically zero at low methane conversions ($< 25\%$), where oxygen is not fully consumed (Dissanayake et al., 1991). It is generally accepted that the direct scheme is followed in the case of Rh and Pt catalysts under conditions of high temperature ($\sim 1{,}000°C$) and very short contact times, as Schmidt and coworkers have shown (Hickman and Schmidt, 1993a) and Fathi et al. (1998).

Most catalysts seem to favor the indirect scheme at intermediate temperatures ($\sim 700–800°C$). A notable exception has been found to be the catalytic systems based on Ru/TiO_2 (Boucouvalas et al., 1996a,b). More specifically, it has been found that, in the absence of significant mass- and heat-transfer resistances, high selectivity to synthesis gas ($\sim 60\%$) is obtained over Ru/TiO_2 catalysts in the low methane conversion range (oxygen conversion $< 100\%$), at temperatures as low as 600–700°C. On the other hand, very low selectivity to synthesis gas is obtained when oxygen conversion is less than 100%, over supported metal catalysts (Ni, Rh, Pd, and Ir), as well as Ru catalysts supported on carriers other than TiO_2 (Boucouvalas et al., 1996b). The extent of the direct scheme was also found to be sensitive to modifications of the

TiO_2 carrier (Boucouvalas et al., 1996a). Doping of the TiO_2 carrier with cations of lower valence, such as Ca^{2+}, was found to promote further the direct formation of synthesis gas over Ru catalysts.

Although mechanistic studies of partial oxidation of methane over Ru catalysts are scarce, studies of the reaction mechanism over Ni, Rh, and Pt catalysts have been carried out by several investigators employing dynamic techniques such as pulse and TAP experiments. Pulse studies over supported Ni catalysts (Au et al., 1994, 1996; Hu and Ruckenstein, 1995) indicate that direct formation of CO takes place over reduced Ni sites via a pyrolysis mechanism, while CO_2 is produced by subsequent oxidation of CO. Oxidation of CO is strongly favored over oxidized Ni.

Regarding Rh catalysts, Buyevskaya et al. (1994, 1996) have investigated the partial oxidation of methane over Rh/γ-Al_2O_3 and Rh-black catalysts in a TAP reactor. Their results indicate that CO_2 is a primary product of the reaction of carbon deposits with lattice oxygen, while CO is formed by the reverse Boudouard reaction, as well as by the reaction of CH_x species with OH surface groups (Buyevskaya et al., 1994). The product distribution is strongly affected by the degree of surface reduction. Wang et al. (1996) and Au and Wang (1997) have performed studies of the reaction over Rh/γ-Al_2O_3 and Rh/SiO_2 catalysts. They have found that selectivity to synthesis gas depends on the concentration of adsorbed oxygen. Total oxidation of methane was found to take place over an oxidized Rh surface (Rh^{3+}), while decomposition of methane and formation of synthesis gas took place over reduced Rh. Deuterium isotope experiments showed that methane dissociation is a slow step, and CO and CO_2 are formed via common intermediates. The partial oxidation of methane over Rh and Pt sponges has been investigated by Mallens et al. (1997) in a TAP reactor. A Mars-Van Krevelen mechanism has been proposed, in which methane reduces the metal oxide, which is reoxidized by gas-phase oxygen. CO and H_2 are primary products of the reaction, while formation of CO_2 and H_2O takes place via consecutive oxidation of CO and H_2.

The only kinetic model for the partial oxidation of methane to synthesis gas that has appeared in the literature, is the one of Hickman and Schmidt (1993b) referring to high-temperature reaction over Rh and Pt surfaces. In the present work, the kinetics of the partial oxidation of CH_4 have been investigated under steady-state conditions as a function of temperature and the partial pressures of CH_4 and O_2. The catalyst employed consists of Ru dispersed on TiO_2 doped with Ca^{+2}, at the level of 0.95 atom %. It has been reported previously that Ru/TiO_2 catalysts promote, in part, the direct formation of synthesis gas in the presence of gas-phase oxygen. The direct route of synthesis gas formation is enhanced upon doping TiO_2 with Ca^{+2} cations. A kinetic model has been developed, which provides good fitting of the experimental kinetic data of the Ru/TiO_2 catalyst.

Experimental Studies

Catalyst preparation

The parent titania carrier used in the present study was obtained from Degussa (P-25). The doped TiO_2 carrier was prepared by the following method: weighted amounts of TiO_2 and CaO (2 wt. %), were slurried with distilled water and thoroughly mixed. The water was evaporated under continuous stirring and the residue was dried at 110°C for 24 h. The dried residue was then powdered and sieved and was heat-treated in the presence of air as follows: the material was heated to 900°C with a heating rate of 4°C/min. It was maintained at 900°C for 5 h and then slowly cooled (approximately 10°C/min) to room temperature.

The Ru catalyst was prepared by the method of incipient wetness impregnation of the support with appropriate amounts of an aqueous solution of ruthenium nitrosyl nitrate of concentration in Ru metal of 10 mg/cm^3. The Ru content of the catalyst was 0.3 wt. %. The impregnated support was dried at 110°C for 24 h. The dried material was then powdered and sieved and placed in a stainless-steel tube for reduction. The material was heated to 200°C with a heating rate of 5°C/min under nitrogen flow ($\sim$ 50 cm^3/min). The flow was then switched to H_2 ($\sim$ 50 cm^3/min) and the material was maintained at 200°C for l h; temperature was then raised to 300°C with the same heating rate and was maintained at this level for l h under H_2 flow. The flow was then switched to N_2 and the catalyst was slowly cooled to room temperature and stored in air-tight vials until further use.

The specific surface area of the catalyst was determined by nitrogen physisorption and was found to be 12 m^2/g. Metal dispersion of the reduced catalyst was estimated by extrapolation of the linear part of the H_2 chemisorption isotherm at 25°C to zero pressure, and was found to be 0.5 (50%). Based on this measurement, the mean diameter of the Ru particles dispersed on TiO_2 is estimated to be 30 Å.

Kinetic measurements

Kinetic measurements were performed under differential conditions (oxygen and methane conversion less than 10%) in the temperature range of 700–800°C, at a total pressure of 1 atm, employing dilute $CH_4/O_2/N_2$ feeds. Nitrogen was used as a diluent instead of helium in order to be able to analyze the produced hydrogen by gas chromatography. The reactor, which is shown in Figure 1, was a quartz tube of an outer diameter of 6 mm. An enlargement of 8 mm at the central part of the tube contained the catalyst bed, which was supported by quartz wool. The quantity of catalyst used was 10–30 mg. The catalyst particle size was in the range of 0.12–0.18 mm. A type K thermocouple enclosed in a quartz thermowell of 3 mm OD was positioned inside the catalyst bed for accurate measurement of catalyst temperature. Mixing conditions in the catalyst bed were estimated by calculation of the axial Peclet number. The Peclet number was found to be of the order of $\sim$ 5. This implies that the catalyst bed can be approximated as two or three CSTRs in series.

Two gas chromatographs were used for the analysis of reactants and products. CH_4 and CO_2 were separated in a Carboxen 1000 column and O_2, N_2, and CO in a Molecular Sieve 5A column, with He as carrier gas, while hydrogen was analyzed in a second chromatograph employing N_2 as the carrier gas. H_2O produced in the reaction was condensed in a condenser located downstream of the reactor.

Kinetic experiments were conducted by varying the partial pressure of one reactant, while keeping the partial pressure of the other reactant constant. The percentage of nitrogen at

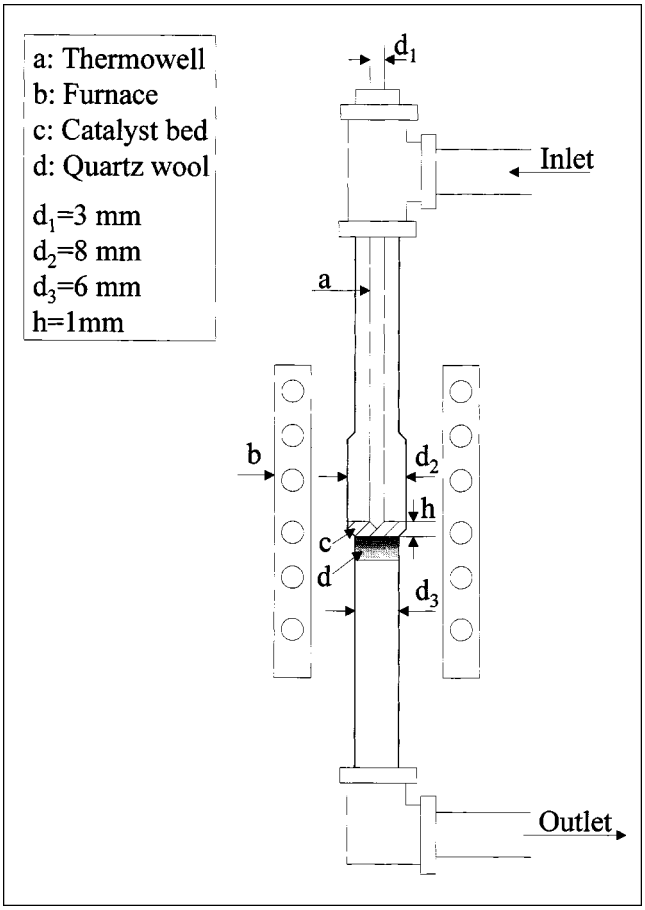

Figure 1. Laboratory-scale reactor for the reaction of partial oxidation of methane.

the reactant mixture was varied in order to keep constant the total flow at each kinetic experiment. The total feed flow rate was generally in the range of 800–1,000 cm^3 (STP)/min. Kinetic experiments were conducted at constant partial pressures of methane and oxygen of 6.4 and 2.7 kPa, respectively, at the temperatures of 700, 750 and 800°C. Whenever a fresh catalyst sample was used, it was initially exposed to an undiluted reaction mixture at 800°C for 12 h. Three different catalyst samples were used for the kinetic measurements, all obtained from the same catalyst batch. The stability of the catalyst has been verified by separated tests lasting up to five days on stream.

The procedure followed prior to kinetic measurement was the following: (a) treatment of the catalyst with H_2 at 300°C for 1 h; (b) increase of temperature to 650°C under N_2 flow; (c) ignition of the catalyst with introduction of 130 cm^3/min of a CH_4/O_2 mixture of 2:1 ratio (methane was introduced first, followed by oxygen after a few seconds); (d) increase of N_2 flow in small steps until a total flow of 800 cm^3/min is obtained; (e) fine-tuning of the feed composition and the furnace temperature of the desired value for the kinetic test.

Results

Mass and heat transport effects

The experimental window, in which valid kinetic measurements can be obtained, is quite limited in the case of highly exothermic oxidation reactions, such as the reaction of partial oxidation of methane. In particular, it is difficult to avoid the existence of interparticle heat-transfer resistances, which cause the temperature of the catalyst particle to increase.

Analytical expressions for the estimation of concentration and temperature differences between gas phase and catalyst surface have been developed (Smith, 1981). These differences permit assessment of the effect of physical processes on the global catalytic rate of reaction, and they can be established from mass and energy balances on the catalyst particle at steady state.

The experimental and calculated parameters used for the theoretical analysis of the mass- and heat-transfer resistances are summarized in Table 1. The experiments were realized at rather low reaction temperatures ($\sim$700–800°C) with very dilute CH_4/O_2 feeds, high feed flow rates ($\sim$800–1,000 cm^3/min), low metal loading in the catalyst (0.3 wt. %), and small mass of the catalyst in the laboratory reactor (10–30 mg). Under these conditions, the calculated difference in CH_4 concentration between the gas phase and the catalyst surface is: $\Delta C < 0.001389$ mol/m^3. Accordingly, the fractional concentration difference $(C_b - C_s)/C_b$ is less than 0.2%. The temperature difference between the gas phase and the catalyst surface is estimated to be $\Delta T < 1.4$ K. Regarding internal

Table 1. Parameters Used for the Estimation of Mass- and Heat-Transfer Resistances

Experimental Parameters	Value	Calculated Parameters*	Value
Pressure, P_t	1 atm	Viscosity, μ	4.2×10^{-5} kg/m·s
Int. reactor diam., d	0.004 m	Gas density, ρ_f	0.32 kg/m^3
Particle diameter, dp	0.00015 m	Heat capacity, c_p	35.2 J/mol·K
External catal. area, a_m	4×10^4 m^{-1}	Thermal conductivity, λ	4 J/s·m·K
Gas velocity, u_o	1.72 m/s	Diffusivity, CH_4-mix.	1.89×10^{-4} m^2/s
Molar volume, V_m	8.9×10^{-2} m^3/mol	**Knud. diff. coef. CH_4	1.7×10^{-3} m^2/s
Reaction rate, r	0.1 mol_{O_2}/kg_c·s	Effective diffusivity, D_{eff}	1.08×10^{-4} m^2/s
Tortuosity, τ	5	Reaction enthalpy, $-\Delta H_r$	255 kJ/mol O_2
Bed porosity, ϵ	0.2–0.4	Mass transf. coeff., k_g	4.93 m^3/m^2·s
†Activation energy, E	48,000 J/mol	Heat transf. coeff., h	1,709 J/s·m^2·K

*Gas-phase parameters have been estimated with methods found in *The Properties of Gases and Liquids*, R. C. Reid, J. M. Prausnitz, and B. E. Poling, McGraw-Hill, New York, 1987.
**Knudsen diffusion coefficient is calculated using an average CH_4 molecular diameter 3.2×10^{-10} m and an average pore radius 2.95×10^{-6} m.
†Activation energy has been found experimentally (Elmasides et al., 1998).

mass and heat transfer resistances, the following criteria have been examined:

Isothermal Concentration Gradient Criterion. Assuming irreversible reaction with reaction order of CH_4 $n = 1$,

$$\frac{\left(\frac{n+1}{2}\right) r \left(\frac{d_p}{6}\right)^2}{D_{\text{eff}} \frac{P_{CH_4}}{P_t V_m}} < 0.25.$$

The effective diffusion coefficient D_{eff} was estimated for Knudsen diffusion, D_k, and molecular diffusion, D_{CH_4-m}. The diffusivity D_{CH_4-m} was calculated using the Stefan-Maxwell equation for ideal gas mixtures ($CH_4/O_2/N_2$).

The isothermal concentration gradient criterion is satisfied, as the estimated value is 0.02, which is sufficiently less than 0.25.

Internal Temperature Gradient Criterion. The criterion employed to assess internal temperature gradients is the following:

$$\frac{(-\Delta H_r) r (d_p/3)^2 \gamma}{\lambda T} < 1,$$

where $\gamma = (E/RT)$, r is the reaction rate, and λ is the thermal conductivity of the reaction mixture. This criterion is also satisfied, since it was calculated to be 0.003, which is sufficiently less than 1.

Kinetic model

Elementary Steps.

1. Formation of carbon and oxygen surface species:

$$CH_4 + S_1 \xrightarrow{1} I \longrightarrow C - S_1 + 4H - S_1 \qquad R_{CH_4} = k_1 P_{CH_4} \theta_{S_1} \tag{5}$$

$$O_2 + 2S_2 \overset{2}{\rightleftharpoons} 2S_2^* \tag{6}$$

$$O_2 + 2S_2^* \overset{3}{\rightleftharpoons} 2O - S_2^*. \tag{7}$$

Methane is assumed to adsorb dissociatively and irreversibly toward formation of surface carbon and adsorbed hydrogen atoms, on specific surface sites designated as S_1. Methane dissociation occurs readily on transition metals, and especially on Rh, Ni, and Ru, and has been studied both theoretically and experimentally (Liao and Zhang, 1998; Au et al., 1998; Wang et al., 1998; Carstens and Bell, 1996; Wu and Goodman, 1994; Nielsen et al., 1995). Adsorption of oxygen is assumed to take place on different active sites (designated as S_2) in a two-step equilibrium process: initial adsorption of oxygen leads to formation of oxidized sites (denoted as S_2^*); subsequent adsorption of oxygen on these sites leads to the formation of the active $O-S_2^*$ species.

2. CO and CO_2 production:

$$C - S_1 + O - S_2^* \xrightarrow{4} CO - S_1 + S_2^* \qquad R_{CH_4} = k_4 \theta_C \theta_O \tag{8}$$

$$CO + S_1 \overset{5}{\rightleftharpoons} CO - S_1 \tag{9}$$

$$CO - S_1 + S_2 \xrightarrow{6} CO - S_2 + S_1 \qquad R_{CO_2} = k_6 \theta_{CO} \theta_{S_2} \tag{10}$$

$$CO - S_2 + O - S_2^* \xrightarrow{7} CO_2 + S_2 + S_2^*. \tag{11}$$

It is proposed that CO is a primary product of the reaction between surface carbon and oxygen. Adsorbed CO is assumed to be in equilibrium with gas phase CO. Carbon dioxide is produced via subsequent oxidation of CO, following its readsorption on sites S_2. Methane dissociation (Eq. 5) and the surface reaction between carbon and adsorbed oxygen atoms (Eq. 8) are assumed to be the rate-determining (slow) steps for formation of adsorbed CO.

3. H_2 and H_2O production:

$$H_2 + 2S_1 \overset{8}{\rightleftharpoons} 2H - S_1 \tag{12}$$

$$H - S_1 + S_2 \xrightarrow{9} H - S_2 + S_1 \qquad R_{H_2O} = k_9 \theta_H \theta_{S_2} \tag{13}$$

$$H - S_2 + O - S_2^* \xrightarrow{10} HO - S_2 + S_2^* \tag{14}$$

$$H - S_2 + HO - S_2 \xrightarrow{11} H_2O + 2S_2. \tag{15}$$

Gas-phase hydrogen is produced by recombination of two hydrogen atoms adsorbed at S_1 sites (step 12), while H_2O is the product of the surface reaction between atomic hydrogen and oxygen (steps 13–15) at sites S_2, with step 13 being rate-determining. Step 12 is assumed to be in equilibrium.

It must be noted that the elementary steps denoted without reverse direction are assumed not to be at equilibrium.

Steam and CO_2 reforming, as well as the water gas shift reaction (WGS), have not been included in the preceding mechanistic scheme. This decision was based on previous work in this laboratory (Elmasides et al., 1998). More specifically, it was found that when CO_2 or H_2O are coadded in the CH_4/O_2 feed, reforming and WGS reactions do not take place at a rate high enough to influence the product distribution of the reaction. The insignificance of reforming reactions under the present experimental conditions has also been confirmed by isotopic transient experiments (Boucouvalas et al., 1996a).

Surface Species Mass Balances.

$$S_1 \text{ sites: } \theta_{S_1} + \theta_C + \theta_{CO} = 1 \tag{16}$$

$$S_2 \text{ sites: } \theta_{S_2} + \theta_O = 1. \tag{17}$$

It is assumed that the surface coverage of total oxidation products (CO_2, H_2O), as well as of hydrogen, is negligible. This is justified by the high reaction temperature and by the low concentration of CO_2 and H_2O (differential conditions). Regarding S_2 sites, it is assumed that the surface concentration of S_2^* sites, as well as of CO adsorbed on S_2 sites, is negligible. The fact that the surface concentration of S_2^* is negligible has been confirmed by *in situ* XPS studies that show that the vast majority of the Ru surface is in the reduced state (Elmasides et al., 1999).

Coverage of Surface Species.

S_1 sites:

$$\theta_C = \frac{k_1}{k_4 K} \frac{P_{CH_4}}{P_{O_2}} \left(1 + K P_{O_2}\right) \theta_{S_1} \tag{18}$$

$$\theta_{CO} = K_5 P_{CO} \theta_{S_1} \tag{19}$$

$$\theta_H = K_8^{1/2} P_{H_2}^{1/2} \theta_{S_1} \tag{20}$$

$$\theta_{S_1} = \frac{k_4 K P_{O_2}}{k_4 K P_{O_2} + k_4 K_5 K P_{O_2} P_{CO} + k_1 P_{CH_4} + k_1 K P_{CH_4} P_{O_2}}. \tag{21}$$

S_2 sites:

$$\theta_O = K P_{O_2} \theta_{S_2} \qquad K = \sqrt{K_2 K_3} \tag{22}$$

$$\theta_{S_2} = \frac{1}{1 + K P_{O_2}}. \tag{23}$$

Based on the preceding equations, the rate of CH_4 consumption is given by Eq. 24:

$$R_{CH_4} = \frac{k_1 k_4 K P_{CH_4} P_{O_2}}{k_4 K P_{O_2} + k_4 K_5 K P_{O_2} P_{CO} + k_1 P_{CH_4} + k_1 K P_{CH_4} P_{O_2}}, \tag{24}$$

while the rate of CO_2 production is given by Eq. 25:

$$R_{CO_2} = \frac{k_4 k_6 K_5 K P_{CO} P_{O_2}}{(1 + K P_{O_2})(k_4 K P_{O_2} + k_4 K_5 K P_{O_2} P_{CO} + k_1 P_{CH_4} + k_1 K P_{CH_4} P_{O_2})}. \tag{25}$$

Based on the carbon balance of the partial oxidation reaction, the rate of CO production is simply the difference between the rates of CH_4 consumption and CO_2 production:

$$R_{CO} = R_{CH_4} - R_{CO_2}. \tag{26}$$

In an analogous manner, the rate of H_2O production is found to be

$$R_{H_2O} = \frac{(1/2) k_4 k_9 K_8^{1/2} K P_{H_2}^{1/2} P_{O_2}}{(1 + K P_{O_2})(k_4 K P_{O_2} + k_4 K_5 K P_{O_2} P_{CO} + k_1 P_{CH_4} + k_1 K P_{CH_4} P_{O_2})}. \tag{27}$$

The 1/2 factor in the numerator of Eq. 27 results from the stoichiometry of H_2O formation (the rate of H_2O formation is half the rate of the surface reaction step represented by Eq. 13). The rate of H_2 production is the difference between the rates of CH_4 consumption and H_2O production:

$$R_{H_2} = 2 R_{CH_4} - R_{H_2O}. \tag{28}$$

Estimation of kinetic parameters

Equations 24 through 28 have been fitted to the experimental kinetic data using the Marquardt-Levenberg algorithm (Marquardt, 1963). A first estimation of the parameters K, K_5, k_6 as well as, of the activation energy E_6 and adsorption enthalpies ΔH_0, ΔH_5, have been obtained from a separate kinetic study of CO oxidation on Ru/TiO_2 at 700°C, assuming that the same mechanism for CO oxidation as the one presented here is applicable. These values have been used as initial parameters for the regression analysis of the present model at 700°C.

The prediction of the activation energies and adsorption enthalpies was done using the kinetic data obtained at all three temperatures at which experiments were performed (total number of data was $N = 70$), via the following relations:

$$k_i = k_{i,T} \exp\left[-\frac{E_i}{R}\left(\frac{1}{T} - \frac{1}{T_r}\right)\right] \qquad i = 1,4,6 \tag{29}$$

$$K_j = K_{j,T} \exp\left[-\frac{\Delta H_j}{R}\left(\frac{1}{T} - \frac{1}{T_r}\right)\right] \qquad j = O_2, CO, \tag{30}$$

where $T_r = 973$ K and $k_{i,T}$, $K_{j,T}$ the rate and equilibrium constants, respectively, of the corresponding elementary reactions at 973 K.

The preexponential factors k_{io}, K_{jo} were calculated from the $k_{i,T}$, $K_{j,T}$, and E_i and ΔH_j values by the Arrhenius and van't Hoff equation:

$$k_{io} = k_{i,T} \exp\left(\frac{E_i}{RT}\right)$$

$$K_{jo} = K_{j,T} \exp\left(\frac{\Delta H_j}{RT}\right).$$

The validity of the calculated parameters was tested by means of the coefficient of determination, R^2, and the F and t statistical tests. The t value is the ratio of the regression coefficient to its standard error. When t values are large, the independent variable can be used to predict the dependent variable.

The F test gauges the contribution of the independent variables in predicting the dependent variable. It is the ratio of the mean squares due to the regression (the sum of squares of the predicted responses divided by the number of parameters) and the mean residual squares (the sum of residual squares divided by the degree of freedom of residuals which is the number of experiments minus the number of parameters). The independent variables contribute to the prediction of the dependent variable when the F value is a large number.

The predicted values of model parameters are shown in Table 2. It can be observed that standard errors are at least one order of magnitude smaller than the estimated values of kinetic parameters. This implies that there is very small uncertainty in the estimation of the coefficients. The F and t values are large enough, which allows one to conclude that the independent variables contribute to the prediction of the dependent variables. Furthermore, these values are larger for activation energies and adsorption enthalpies as a consequence of the bigger number of experiments used ($N = 70$).

Using the predicted values of model parameters, the statistical significance of the adsorption and reaction constants at 750 and 800°C was tested (Table 3).

Table 2. Values of Model Parameters

T (°C)	k_1 (mol/g·s·kPa)	k_4 (mol/g·s)	K (kPa^{-1})	K_5 (kPa^{-1})	k_6 (mol/g·s)	F	R^2
700	$(3.37\pm0.09)\times10^{-5}$	$(3.9\pm0.06)\times10^{-3}$	$(1.65\pm0.025)\times10^{-2}$	0.28 ± 0.013	$(6.5\pm0.3)\times10^{-4}$		
t	39.4	60.7	58.6	18.8	18	131	
	$E_1=27\pm0.5$ (kJ/mol)	$E_4=206\pm0.2$ (kJ/mol)	$\Delta H_o=-172\pm0.1$ (kJ/mol)	$\Delta H_5=-173\pm0.1$ (kJ/mol)	$E_6=116\pm0.8$ (kJ/mol)		>0.99
t	86.7	660.8	552.3	771.4	573.9	293	
	$k_{10}=9.5\times10^{-4}$	$k_{40}=4.5\times10^{8}$	$K_0=9.6\times10^{-12}$	$K_{50}=1.4\times10^{-10}$	$k_{60}=1.1\times10^{3}$		

Only the product $(K_8^{1/2}k_9)$, and not the individual constants, were determined. No statistically significant values were obtained for K_8 and k_9, because there is no term containing these constants in the denominator of the rate Eq. 27. Hence the product $k_9K_8^{1/2}$ was determined by Eq. 27 using the values of the other kinetic parameters estimated from Eqs. 24 and 25. The values for the product $k_9K_8^{1/2}$ at temperatures of 700, 750 and 800°C are 1.6×10^{-4}, 1.5×10^{-4}, and 1.85×10^{-4} mol/g·s·kPa, respectively.

Thermodynamic consistency of the kinetic parameters

The value of preexponential factors of rate constants can be used to estimate the validity of presumed elementary steps. For adsorption equilibrium constants $K=\exp(\Delta S_a^o/R)\exp(\Delta H_a^o/RT)$, the rule is that ΔH_a^o should be negative, as adsorption is in general exothermic, while entropy normally decreases upon adsorption, although the loss cannot exceed the entropy of the fluid phase molecule, S_{fluid}^o (Boudart and Djega-Mariadassou, 1984): $0<-\Delta S_a^o<S_{\text{fluid}}^o$. This inequality can be converted to the following:

$$\text{(i)}\quad \Delta S_a^o<0 \quad \text{or} \quad \exp(\Delta S_a^o/R)=K_{jo}<1 \tag{31}$$

$$\text{(ii)}\quad -\Delta S_a^o<S_{\text{fluid}}^o \quad \text{or} \quad \exp(\Delta S_a^o/R)=K_{jo}>\exp(-S_{a,g}^o/R). \tag{32}$$

The preexponential factor of the CO adsorption constant is $K_{50}=1.4\times10^{-8}$ ($P=1$ atm) and the $S_{\text{CO},g}^o$ value at 25°C is 198.5 J/(mol·K). Thus, the preceding rules are satisfied:

$$\text{(i)}\quad K_{50}=1.4\times10^{-8}<1$$

$$\text{(ii)}\quad K_{50}=1.4\times10^{-8}>4.25\times10^{-11}=\exp(-S_{a,g}^o/R).$$

As a guideline, there is one more rule, which can be summarized as follows (Vannice et al., 1979):

$$\text{(iii)}\quad 10\le-\Delta S_a^o\le12.2-0.0014\Delta H_a^o. \tag{33}$$

The lower limit was established by estimating the loss of free volume upon adsorption at the standard-state coverage of $\theta=1/2$, while the upper limit was a comparison between entropies of chemisorption obtained from the literature and a linear relationship between ΔS_a^o and ΔH_a^o for physical adsorption.

Since $-\ln K_{jo}=-\Delta S_a^o/R$, the inequality of Eq. 33 can be written in the following form:

$$10/R\le-\ln K_{jo}\le(12.2-0.0014\Delta H_a^o)/R$$

or

$$1.2\le-\ln K_{50}=18.1\le30.6.$$

Thereupon, this criterion is satisfied for CO adsorption.

Regarding oxygen adsorption, the parameter K_O incorporates both elementary steps of oxygen adsorption:

$$K_O=\sqrt{K_{2O}K_{3O}}=\exp\left(\frac{\Delta S_2+\Delta S_3}{2R}\right)=9.6\times10^{-10}\quad \text{atm}^{-1}.$$

Therefore, it is not feasible in this case to check the equilibrium constants separately, but it is obvious that the same inequalities can be used for the sum of the entropy and enthalpy changes of the elementary steps 6 and 7:

$$\text{(i)}\quad \Delta S_2+\Delta S_3<0 \quad \text{or} \quad \exp\left(\frac{\Delta S_2+\Delta S_3}{2R}\right)=K_O<1.$$

$$\text{(ii)}\quad -(\Delta S_2+\Delta S_3)<2S_{O_2,g}^o=410\ \text{J/mol·K}$$

or

$$\exp\left(\frac{\Delta S_2+\Delta S_3}{2R}\right)=K_O>\exp\left(-\frac{S_{O_2,g}^o}{R}\right)=1.95\times10^{-11}.$$

$$\text{(iii)}\quad 20\le-(\Delta S_2+\Delta S_3)\le24.4-0.0028\Delta H_O$$

or

$$1.2\le-\ln K_O=20.8\le30.4.$$

Table 3. Parameter Estimates from the Model at 750° and 800°C

T (°C)	k_1 (mol/g·s·kPa)	k_4 (mol/g·s)	K (kPa^{-1})	K_5 (kPa^{-1})	k_6 (mol/g·s)	F	R^2
750	$(3.9\pm0.4)\times10^{-5}$	$(1.36\pm0.08)\times10^{-2}$	$(5.8\pm0.3)\times10^{-3}$	0.09 ± 0.01	$(1.3\pm0.2)\times10^{-3}$		
t	45	58	44	22	32	140	
800	$(4.2\pm0.2)\times10^{-5}$	$(4.2\pm0.1)\times10^{-2}$	$(2.3\pm0.1)\times10^{-3}$	0.037 ± 0.01	$(2.5\pm0.9)\times10^{-3}$		>0.99
t	52	51	50	23	19	151	

Table 4. Calculated Values of Sticking Coefficient of Methane

T, (°C)	700	750	800
$k_1 = (\text{mol}\cdot\text{s})/(\text{g}\cdot\text{cm})$	4.64×10^{-13}	5.26×10^{-13}	5.94×10^{-13}
s	1.32×10^{-6}	1.85×10^{-6}	2.48×10^{-6}

The thermodynamic criteria are satisfied; also in the case of oxygen adsorption. Although the thermodynamic criteria were examined for the sum of the entropy changes of the elementary steps 6 and 7, the value of this sum is far enough from the limits established by thermodynamics.

Estimation of CH_4 sticking coefficient

According to the kinetic theory, the adsorption coefficient of methane, k_1, can be expressed as follows:

$$K_1 = \frac{s_o \exp(-E/RT)}{\sqrt{2\pi M_{CH_4} R_g T}}. \qquad (34)$$

The numerator term, $s_o \exp(-E/RT)$, corresponds to the sticking coefficient of methane, s. Calculated values of s via this relationship are presented in Table 4. The sticking coefficient of methane is in the range of 10^{-6}, and it almost doubles with an increase in reaction temperature from 700°C to 800°C. The weak dependence of the sticking coefficient on temperature is due to the low activation energy of methane dissociation, as analyzed in the Discussion section.

Experimental results

The effect of methane partial pressure on the rates of CO, CO_2, H_2, and H_2O production and of CH_4 consumption at the reaction temperature of 700°C and constant oxygen partial pressure of 2.7 kPa is shown in Figure 2 (experimental points). The rates of CO and H_2 production increase with increasing methane pressure (that is, with increasing CH_4/O_2 ratio), while the rates of CO_2 and H_2O production exhibit a slight decline with increase in methane pressure. Overall, the reaction order with respect to methane pressure is positive, tending toward saturation at high methane pressures in accordance with Eq. 24.

The effect of oxygen partial pressure on the rates of CO, CO_2, H_2 and H_2O production and of CH_4 consumption at the reaction temperature of 700°C and constant methane partial pressure of 6.4 kPa is shown in Figure 3 (experimental points). It can be seen that the reaction order with respect to oxygen is positive and that the selectivity toward synthesis gas is very high at low oxygen pressures (that is, at high CH_4/O_2 ratios) and decreases with increasing oxygen pressure.

Kinetic experiments have also been performed at integral conditions. The effect of space velocity on CH_4 conversion and CO and H_2 selectivity is presented in Figure 4. For CH_4 conversions up to 25% (where oxygen conversion is less than 100%), CO and H_2 selectivities remain practically constant. When the partial oxidation of methane is proceeding via the indirect scheme (reactions 2, 3, 4), then CO and H_2 selectivities should decrease with increasing space velocity (Dissanayake et al., 1991; Nakagawa et al., 1998; Van Looij et al., 1994). The constant selectivities observed in the present study

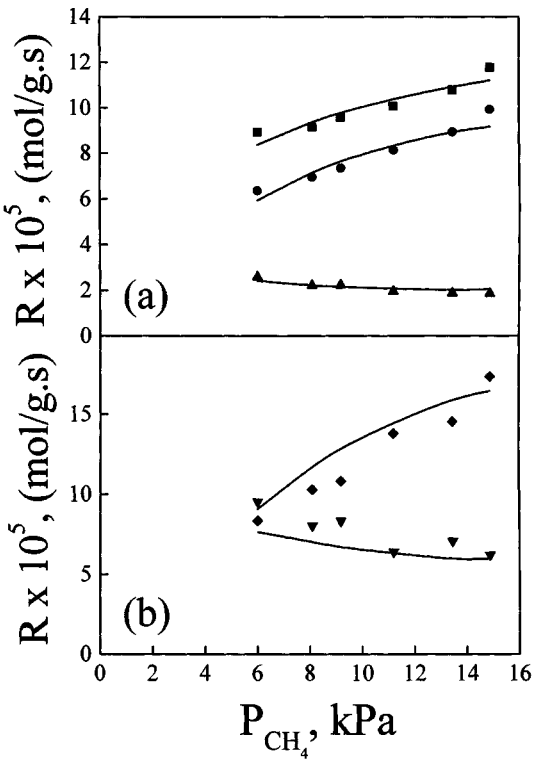

Figure 2. Influence of methane partial pressure on the rates of (a) CO (●) and CO_2 (▲) production and CH_4 (■) consumption, and (b) H_2 (◆) and H_2O (▼) production, under CPO conditions with constant oxygen partial pressure of 2.7 kPa and temperature $T = 700$°C (solid lines: model; symbols: experimental data).

(Figure 4) with variation of space velocity implies that CO and H_2 are the primary products of the reaction.

Quality of fitting of the kinetic model

The model prediction is presented in Figures 2 and 3, in the form of continuous lines for the rates of CH_4 consumption and CO, CO_2, H_2, and H_2O production under conditions of variable partial pressure of CH_4 (Figure 2) or variable partial pressure of O_2 (Figure 3) at 700°C. The kinetic model satisfies well the experimental observations.

The predictions of the model for the rate of CH_4 consumption and the rates of CO_2 and CO formation are compared in Figure 5 to the experimental values at all temperatures. It can be observed that the fitting obtained is very satisfactory and that the points are randomly scattered along the $\theta = 45°$ line. The same picture emerges in the case of the rates of H_2O and H_2 formation (Figure 6), with the possible exception of the region of high reaction rates of H_2 formation, where predicted rates are lower than experimental ones.

Estimation of surface coverage under reaction conditions

Figures 7 and 8 show the dependence of carbon and CO surface coverage on the partial pressures of O_2 and CH_4 and temperature, as predicted by the kinetic model. It can be ob-

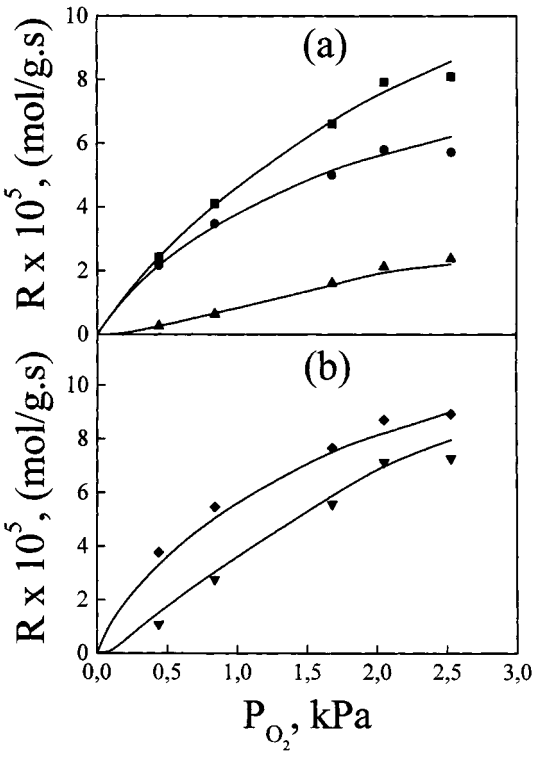

Figure 3. Influence of oxygen partial pressure on the rates of (a) CO (●) and CO_2 (▲) production and CH_4 (■) consumption, and (b) H_2 (♦) and H_2O (▼) production, under CPO conditions with constant methane partial pressure of 6.4 kPa and temperature $T = 700$°C (solid lines: model, symbols: experimental data).

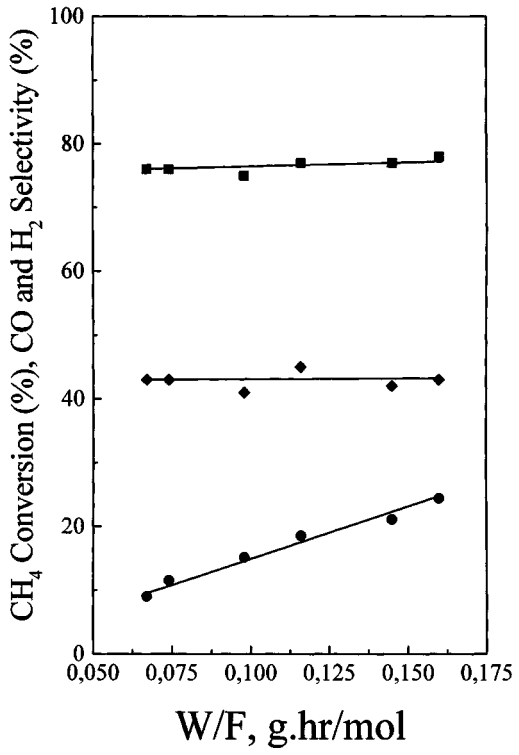

Figure 4. Effect of contact time on the conversion of methane (■), CO selectivity (●), and H_2 selectivity (♦) at $T = 800$°C and $CH_4/O_2 = 6/3$.

served that the main surface species is atomic carbon, whose coverage is in the range of 0.5–0.9. The carbon coverage increases with increase in CH_4 pressure, and decreases with increase in oxygen pressure. On the other hand, carbon coverage decreases slightly with increase of reaction temperature. CO coverage decreases with increasing temperature as expected from adsorption thermodynamics.

Discussion

The performance of the Ru/TiO_2 catalyst is rather unique in the sense that it produces CO and H_2 with high selectivity in the low conversion region (where oxygen is still present in the reaction mixture) and at low temperatures (~ 700°C). Fathi et al. (1998) have reported results of the partial oxidation of methane over Pt and Pt/Rh gauzes under comparable conditions. Employing a CH_4:O_2:Ar mixture of ratio 2:1:10, they found selectivities of CO and H_2 of the order of 50% and $< 5\%$, respectively, at methane conversions of $\sim 15\%$ and a reaction temperature of 700°C. Corresponding results of the Ru/TiO_2 catalyst indicate selectivities of CO and H_2 of the order of $\sim 70\%$ and 50%, respectively.

The only kinetic model that has appeared in the literature for the reaction of partial oxidation of methane, is the one proposed by Hickman and Schmidt (1993b). This model comprises a 19-step reaction mechanism, and it has been used to simulate the partial oxidation of methane over Rh and Pt surfaces, obtaining the reaction-rate parameters from work previously published in the literature. The basic assumptions were that oxygen adsorbs in a noncompetitive fashion with first order kinetics and that methane dissociates irreversibly toward surface carbon and hydrogen. These assumptions have also been used in the present work. Regarding oxygen ad-

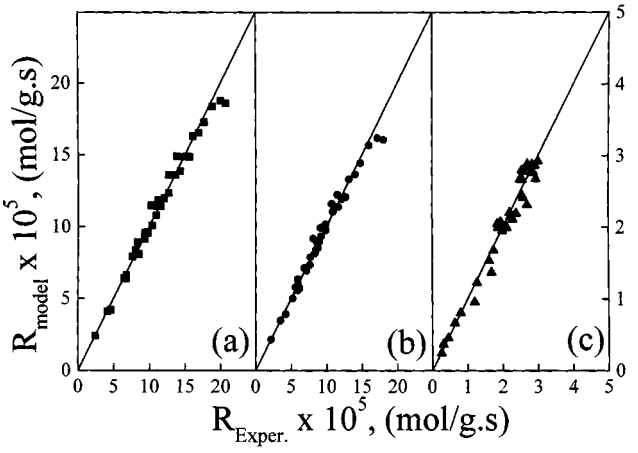

Figure 5. Comparison of experimentally determined reaction rates with model predictions: (a) CH_4 (■) consumption; (b) CO (●); (c) CO_2 (▲) production.

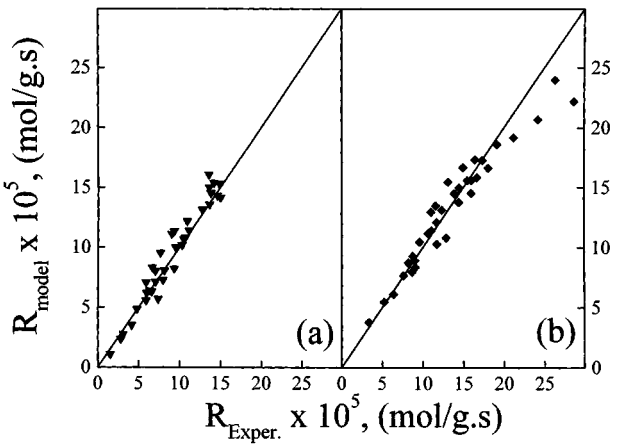

Figure 6. Comparison of experimentally determined reaction rates with model predictions: (a) H_2O (▼); (b) H_2 (♦) production.

sorption, fitting of the kinetic data of Ru/TiO_2 catalyst was poor, if competitive adsorption of oxygen or an adsorption order of 0.5 (dissociative oxygen adsorption) was assumed. For example, the assumption of competitive oxygen adsorption leads to a kinetic model predicting a reaction order of -1 at high methane and oxygen partial pressures. Such a trend was not observed experimentally. First-order oxygen adsorption has been used in many kinetic studies of order oxidation reactions, such as CO oxidation (Oh et al., 1986)

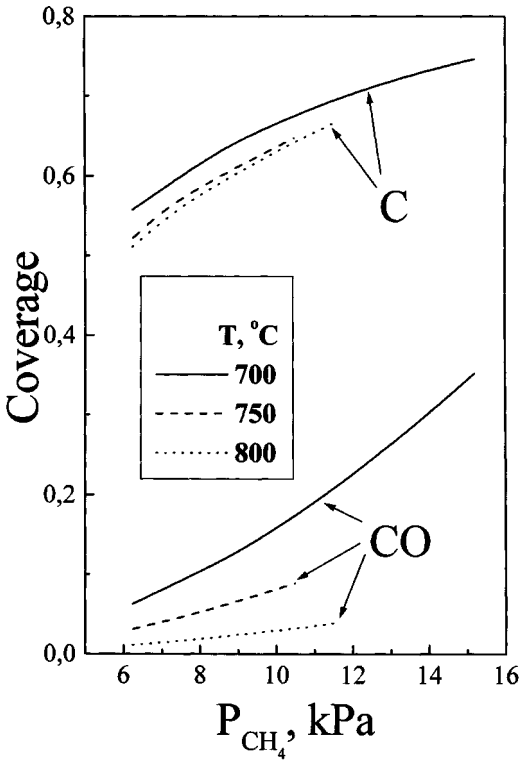

Figure 7. Influence of CH_4 partial pressure on the surface coverage of CO and C.

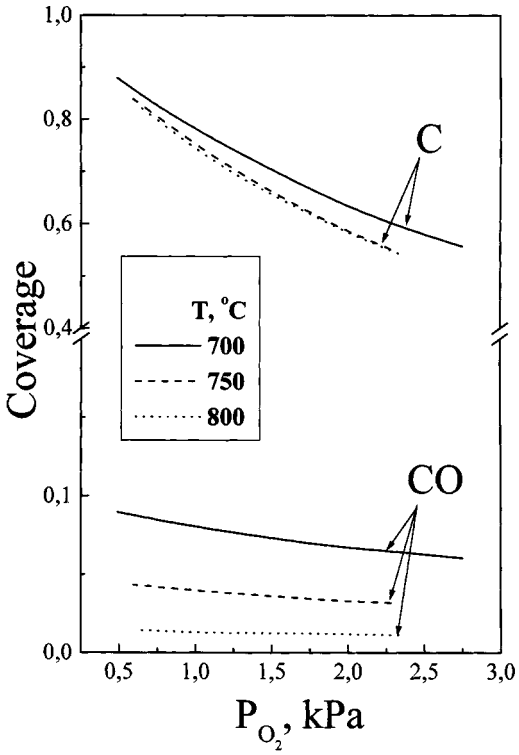

Figure 8. Influence of O_2 partial pressure on the surface coverage of CO and C.

and its physical meaning is that the controlling process of adsorption is the interaction of one oxygen molecule with one active site.

Methane adsorption

Regarding methane adsorption, the assumption of irreversible adsorption is well based on the fact that the coverage of hydrogen atoms is negligible to allow appreciable rates of CH_x ($x = 0-3$) hydrogenation. This is further supported by the finding that fitting of the kinetic data was poor when reversible steps of methane adsorption and dissociation were assumed. The model assumes that methane adsorption is rate-determining and first-order with respect to methane pressure. The estimated value of activation energy of methane dissociation of 27 kJ/mol (Table 2) is in good agreement with results of other investigators. More specifically, Koerts et al. (1992) have determined a value of 26 kJ/mol for methane dissociation over Ru/SiO_2 in the temperature range of 350–500°C. Carstens and Bell (1996) report values of 29 kJ/mol for noncarburized Ru and 24.5 kJ/mol for carburized Ru supported on SiO_2. Wu and Goodman (1994) have measured an activation energy of 35 kJ/mol on single-crystal Ru(0001). Although the activation energy for methane dissociation is not large, adsorption rates are low because of the low sticking coefficient of methane. The value of the sticking coefficient of methane was found to be 1.3×10^{-6} at 700°C (Table 4). Using the activation energy of methane adsorption of 27 kJ/mol (Table 2), the preexponential factor of the sticking coefficient of methane, s_o, is $\sim 4\times10^{-5}$. Wu and Goodman (1994) have measured the sticking coefficient of methane

on Ru(0001). Based on their data, s_o can be estimated to be $\sim 7\times10^{-4}$. Carstens and Bell (1996) have estimated the sticking coefficient of methane on a Ru/SiO_2 catalyst. Their reported values of s_o are in the range of $2.0-5.8\times10^{-7}$, depending on whether Ru is carburized or not. Therefore, the value of s_o found in this work compares well with values reported in the literature.

Oxygen and CO adsorption

Regarding oxygen adsorption, the model developed assumes a two-step adsorption mechanism. During the first step, oxygen interacts with the Ru metallic surface sites, S_2. The assumption of specific sites for O_2 adsorption is based on the fact that oxygen adsorbs on a different ensemble of sites. Au et al. (1998) suggest that atomic oxygen prefers to adsorb on hollow sites of metallic surfaces. The difference between S_1 and S_2 sites could also be attributed to the existence of regions on the metallic surface that interact more strongly with O_2. The interaction of O_2 with S_2 sites creates the oxidized sites, S_2^* (Eq. 6). The active form of oxygen is subsequently formed upon adsorption on such S_2^* sites. There exist indications in the literature in support of this hypothesis. Sommerfeld and Parravano (1965) have studied the chemisorption of O_2 on RuO_2. They proposed that there are sites with different bonding arrangement with O_2. More specifically, they propose that O_2 adsorption on a RuO_2 surface leads to the formation of surface groups $Ru(O)_x$. These surface groups $Ru(O)_x$ are generated by O_2 adsorption on defects in bulk RuO_2.

As far as CO adsorption is concerned, the value of -173 kJ/mol predicted by the model for the heat of adsorption of CO (Table 2) is reasonable. Low and Bell (1979) have found two states of adsorbed CO with corresponding values of activation energy of desorption of 113 and 155 kJ/mol. It is plausible to assume that under the high-temperature conditions of the partial oxidation of methane, only strongly adsorbed CO will be present in the catalyst surface and participate in surface reactions.

C + O reaction

A value of 206 kJ/mol for the activation energy of the C + O reaction has been determined from the fitting of the model to the kinetic data (Table 2). This is in good agreement with activation energies reported for other metals. For example, values in the range of 134–180 kJ/mol have been reported for Ni catalysts (Benziger and Preston, 1984; Kelemen and Krenos, 1985; Astaldi et al., 1989). The activation energy for Ni(111) has been estimated theoretically to be 146 kJ/mol (Shustorovich, 1990). In the case of Pt, an activation energy of 192 kJ/mol has been reported (Kislyuk et al., 1991).

CO + O reaction

A value of 116 kJ/mol for the activation energy of the CO oxidation reaction has been found in this work. Apparent activation energies of the CO oxidation reaction have been found to be 84 kJ/mol for Ru(0001) and 94 kJ/mol for Ru/SiO_2 (Goodman and Peden, 1986). Comparison of the rate constants for the C + O reaction, k_4, and the CO + O reaction, k_6, shows that the former is larger and the difference increases with increasing reaction temperature, for example, the ratio k_4/k_6 is ~ 6 at 700°C and ~ 17 at 800°C. This implies that CO selectivity should increase with temperature. Indeed, employing a $CH_4/O_2/N_2 = 6/3/91$ feed, the CO selectivity was found to be 70%, 75%, and 81% at reaction temperatures of 700, 750 and 800°C, respectively. Therefore, the high selectivity of the Ru catalyst can be attributed to its higher activity in the C + O reaction compared to the one in the CO + O reaction.

The kinetic model of the present work assumes that CO has to readsorb on an S_2 site in order to react with adsorbed oxygen toward CO_2. This assumption was found to provide better qualitative and quantitative description of the experimental kinetic results. It has to be noted, however, that there are currently no experimental findings in the literature in support of this hypothesis.

Conclusions

Kinetic results of the reaction of partial oxidation of methane to synthesis gas over a Ru/TiO_2 catalyst have been fitted successfully with a kinetic model based on the following elementary steps: dissociative adsorption of methane, noncompetitive adsorption of oxygen, primary formation of carbon monoxide and hydrogen, and secondary formation of carbon dioxide and water by subsequent oxidation of carbon monoxide and hydrogen. The values of the model parameters satisfy thermodynamic constraints and are in good agreement with the literature data derived from surface science techniques or kinetic studies of elementary surface processes.

Acknowledgment

Financial support by the Commission of the European Union (Contract no. JOF3-CT95-0026) is gratefully acknowledged.

Literature Cited

Astaldi, C., A. Santoni, F. Della Valle, and R. Rosei, "CO Dissociation and Recombination Reactions on Ni(100)," *Surf. Sci.*, **220**, 322 (1989).

Au, C. T., Y. H. Hu, and H. L. Wan, "Pulse Studies of CH_4 Interaction with NiO/Al_2O_3 Catalysts," *Catal. Lett.*, **27**, 199 (1994).

Au, C. T., H. Y. Wang, and H. L. Wan, "Mechanistic Studies of CH_4/O_2 Conversion Over SiO_2-Supported Nickel and Copper Catalysts," *J. Catal.*, **158**, 343 (1996).

Au, C. T., and H. Y. Wang, "Mechanistic Studies of Methane Partial Oxidation to Syngas Over SiO_2-Supported Rhodium Catalysts," *J. Catal.*, **167**, 337 (1997).

Au, C. T., M.-S. Liao, and C.-F. Ng, "A Detailed Theoretical Treatment of the Partial Oxidation of Methane to Syngas on Transition and Coinage Metal (M) Catalysts (M = Ni, Pd, Pt, Cu)," *J. Phys. Chem. A*, **102**, 3959 (1998).

Benziger, J. B., and R. E. Preston, "Recombination Reactions on Ni(111)," *Surf. Sci.*, **141**, 567 (1984).

Boucouvalas, Y., Z. L. Zhang, A. M. Efstathiou, and X. E. Verykios, "Partial Oxidation of Methane to Synthesis Gas over Ru/TiO_2 Catalysts," *Stud. Surf. Sci. Catal.*, **101**, 443 (1996a).

Boucouvalas, Y., Z. L. Zhang, and X. E. Verykios, "Partial Oxidation of Methane to Synthesis Gas via the Direct Reaction Scheme over Ru/TiO_2 Catalyst," *Catal. Lett.*, **40**, 189 (1996b).

Boudart, M., and G. Djega-Mariadassou, *Kinetics of Heterogeneous Catalytic Reactions*, Princeton Univ. Press, Princeton, NJ (1984).

Buyevskaya, O. V., K. Walter, D. Wolf, and M. Baerns, "Primary Reaction Steps and Active Surface Sites in the Rhodium-Catalyzed Partial Oxidation of Methane to CO and H_2," *Catal. Lett.*, **38**, 81 (1996).

Buyevskaya, O. V., D. Wolf, and M. Baerns, "Rhodium-Catalyzed Partial Oxidation of Methane to CO and H_2. Transient Studies on its Mechanism," *Catal. Lett.*, **29**, 249 (1994).
Carstens, J. N., and A. T. Bell, "Methane Activation and Conversion to Higher Hydrocarbons on Supported Ruthenium," *J. Catal.*, **161**, 423 (1996).
Dissanayake, D., M. P. Rosynek, K. C. C. Kharas, and J. H. Lunsford, "Partial Oxidation of Methane to Carbon Monoxide and Hydrogen over a Ni/Al_2O_3 Catalyst," *J. Catal.*, **132**, 117 (1991).
Elmasides, C., T. Ioannides, and X. E. Verykios, "Kinetic Behaviour of the Ru/TiO_2 Catalyst in the Reaction of Partial Oxidation of Methane," *Stud. Surf. Sci. Catal.*, **119**, 801 (1998).
Elmasides, C., D. I. Kondarides, W. Grunert, and X. E. Verykios, "XPS and FTIR Study of Ru/Al_2O_3 and Ru/TiO_2 Catalysts: Reduction Characteristics and Interaction with a Methane–Oxygen Mixture," *J. Phys. Chem.*, **103**, 5227 (1999).
Fathi, M., K. H. Hofstad, T. Sperle, O. A. Rokstad, and A. Holmen, "Partial Oxidation of Methane to Synthesis Gas at Very Short Contact Times," *Catal. Today*, **42**, 205 (1998).
Goodman, D. W., and C. H. F. Peden, "CO Oxidation over Rh and Ru: A Comparative Study," *J. Phys. Chem.*, **90**, 4893 (1986).
Hickman, D. A., and L. D. Scmidt, "Production of Syngas by Direct Catalytic Oxidation of Methane," *Science*, **259**, 343 (1993a).
Hickman, D. A., and L. D. Schmidt, "Steps in CH_4 Oxidation on Pt and Rh Surfaces: High-Temperature Reactor Simulations," *AIChE J.*, **39**, 1164 (1993b).
Hu, Y. H., and E. Ruckenstein, "Pulse-MS Study of the Partial Oxidation of Methane Over Ni/La_2O_3 Catalyst," *Catal. Lett.*, **34**, 41 (1995).
Kelemen, S. R., and J. Krenos, "Oxidation Studies of Carbided Nickel Surfaces," *Surf. Sci.*, **157**, 491 (1985).
Kislyuk, M. U., V. V. Migulin, V. V. Savkin, A. G. Vlasenko, A. V. Sklyarov, and I. Tretyakov, "Reaction of Oxygen with Carbon on a Platinum Surface and the Spatial Distribution of the Carbon Monoxide Produced," *Kinet. Catal.*, **31**, 1219 (1991).
Koerts, T., M. J. A. G. Deelen, and R. A. van Santen, "Hydrocarbon Formation from Methane by a Low-Temperature Two-Step Reaction Sequence," *J. Catal.*, **138**, 101 (1992).
Liao, M.-S., and Q.-E. Zhang, "Dissociation of Methane on Different Transition Metals," *J. Molec. Catal. A*, **136**, 185 (1998).
Low, G. G., and A. T. Bell, "Studies of CO Desorption and Reaction with H_2 on Alumina-Supported Ru," *J. Catal.*, **57**, 397 (1979).
Mallens, E. P. J., J. H. B. J. Hoebink, and G. B. Marin, "The Reaction Mechanism of the Partial Oxidation of Methane to Synthesis Gas: A Transient Kinetic Study over Rhodium and a Comparison with Platinum," *J. Catal.*, **167**, 43 (1997).
Marquardt, D. W., "An Algorithm for Least Squares Estimation of Parameters," *J. Soc. Ind. Appl. Math.*, **11**, 431 (1963).
Nakagawa, K., N. Ikenaga, T. Suzuki, T. Kobayashi, and M. Haruta, "Partial Oxidation of Methane to Synthesis Gas over Supported Iridium Catalysts," *Appl. Catal. A.* **169**, 281 (1998).
Nielsen, B. O., A. C. Luntz, P. M. Holmblad, and I. Chorkendorff, "Activated Dissociative Chemisorption of Methane on Ni(100): A Direct Mechanism under Thermal Conditions?" *Catal. Lett.*, **32**, 15 (1995).
Oh, S. H., G. B. Fisher, J. C. Carpenter, and D. W. Goodman, "Comparative Kinetic Studies of $CO\text{-}O_2$ and CO-NO Reactions over Single Crystal and Supported Rhodium Catalysts," *J. Catal.*, **100**, 360 (1986).
Pena, M. A., J. P. Gomez, and J. L. G. Fierro, "New Catalytic Routes for Syngas and Hydrogen Production," *Appl. Catal. A*, **144**, 7 (1996).
Shustorovich, E., "The Bond-Order Conservation Approach to Chemisorption and Heterogeneous Catalysis: Application and Implications," *Adv. Catal.*, **37**, 101 (1990).
Smith, J. M., *Chemical Engineering Kinetics*, McGraw-Hill, New York (1981).
Sommerfeld, J. T., and G. Parravano, "Oxygen Chemisorption on Ruthenium Dioxide," *J. Phys. Chem.*, **69**, 102 (1965).
Van Looij, F., J. C. van Giezen, E. R. Stobbe, and J. W. Geus, "Mechanism of the Partial Oxidation of Methane to Synthesis Gas on a Silica-Supported Nickel Catalyst," *Catal. Today*, **21**, 495 (1994).
Vannice, M. A., S. H. Hyun, B. Kalpakci, and W. C. Liauh, "Entropies of Adsorption in Heterogeneous Catalytic Reactions," *J. Catal.*, **56**, 358 (1979).
Wang, D., O. Dewaele, A. M. De Groote, and G. F. Froment, "Reaction Mechanism and Role of the Support in the Partial Oxidation of Methane on Rh/Al_2O_3," *J. Catal.*, **159**, 418 (1996).
Wang, D., O. Dewaele, and G. F. Froment, "Methane Adsorption on Rh/Al_2O_3," *J. Molec. Catal. A*, **136**, 301 (1998).
Wu, M. C., and D. W. Goodman, "High-Resolution Electron Energy-Loss Measurements of Sticking Coefficients of Methane Decomposition on Ru(0001)," *Surf. Sci. Lett.*, **306**, L529 (1994).

Manuscript received Sept. 17, 1999, and revision received Jan. 31, 2000.